Original Research

Atherosclerotic plaque identification by virtual histology intravascular ultrasound in a rabbit abdominal aorta model of vulnerable plaque

Qing-Fei Lin[1,2], Yu-Kun Luo[1], Zi-Wen Zhao[1], Wei Cai[1], Xing-Chun Zhen[1] and Liang-Long Chen[1]

[1]Department of Cardiology, Union Hospital, Fujian Medical University, and Fujian Institute of Coronary Artery Disease, Fuzhou 350001, P. R. China; [2]Department of Cardiology, Wuyishan Municipal Hospital, Fujian Province 354300, China
Corresponding author: Lianglong Chen. Email: lianglong_chen@yahoo.com.cn

Abstract

This study aimed to evaluate the utility of virtual histology intravascular ultrasound (VH-IVUS) for recognizing vulnerable plaque compared to histological pathological analysis. Four-month-old New Zealand rabbits ($n = 16$) were randomly divided into two groups: one fed a high-fat diet and subjected to balloon injury (experimental, $n = 10$) and one fed a high-fat diet alone (control, $n = 6$). Blood lipid profiles of overnight-fasted rabbits were measured at week 2 (beginning of study) and week 12 (end of study). At week 12, experimental group rabbits underwent IVUS under anaesthesia. Rabbits were sacrificed and a 5-cm segment of the abdominal aorta was removed. Arterial sections were subjected to pathological and immunohistochemical analyses. Serum lipid levels increased in all rabbits fed with high-fat diet, with low-density lipid cholesterol (LDL-C) levels increasing the most. Levels of six biomarkers (high sensitivity C-reactive protein, matrix metalloproteinase-3, interleukin [IL]-1, IL-10, tumour necrosis factor-α, and oxidized [ox]-LDL) showed no differences between the two groups at week 2, but were higher in the experimental group at week 12. A total of 276 atherosclerotic plaques in the experimental group were analysed. VH-IVUS had sensitivities of 87% and 92% for detection of noncalcified and calcified thin-cap fibroatheromas, respectively. VH-IVUS correctly identified 85% and 89% of noncalcified and calcified fibroatheromas, respectively. For detection of pathological intimal thickening, VH-IVUS showed a sensitivity of 79% and positive predictive value of 78%. Linear regression analysis showed a strong correlation between histology and VH-IVUS for the percent area of fibrous fibro-fatty tissue, necrotic calcified tissue, and confluent necrotic core. The intra-observer and inter-observer variability of the intimal and medial-adventitial boundaries was low. Endothelial injury followed by a high-fat diet in rabbits is a viable method for inducing atheroma, and VH-IVUS is a feasible, reproducible, and valuable means of vulnerable plaque identification *in vivo*.

Keywords: atherosclerosis, vulnerable plaque, VH-IVUS, intravascular ultrasound, inflammation

***Experimental Biology and Medicine* 2013; 238: 1223–1232. DOI: 10.1177/1535370213493704**

Introduction

Atherosclerosis (AS) is a cardiovascular disease that is associated with high morbidity. The exact cellular and molecular pathogeneses of vulnerable plaques remain unclear, despite ongoing research. Therefore, illustrating the pathogenesis of the vulnerable plaque and exploring methods of stable plaque therapy are of great interest. Such goals may be accomplished through the establishment of experimental animal models similar to human AS. An ideal model should have the following basic features[1]: occurrence and development of AS should be consistent with those in humans; plaque should display vulnerability, with a small fibrous cap/lipid nucleus ratio, many inflammatory cells, and a low collagen content; plaque should rupture spontaneously, with a thrombus rich in platelets and fibrin; the model should be reactive to treatment, and the same treatment should be utilizable for human trials; and the experiment should be reproducible.

Many studies of AS have used a high-fat diet or arterial wall balloon injury rabbit model, or a combination of these methods.[2–4] However, to date, no standard animal model of vulnerable plaque has been established.[5] Vulnerable plaque is mostly confirmed by pathological methods, and the effects of treatment are compared in a horizontal manner. A

vulnerable plaque experimental model is needed in which plaques can be observed in vivo dynamically and vertically. Recently, Rodriguez-Granillo proposed that plaque composition measurements by virtual histology intravascular ultrasound (VH-IVUS) are reproducible,[6] suggesting that dynamic longitudinal studies are feasible with this method.

In the present, short-term study, atherosclerotic plaques were generated in New Zealand white rabbits through use of a high-fat diet combined with arterial intimal injury. The resulting aortic atherosclerotic plaques strongly resembled human atherosclerotic plaques. The aim of this study was to validate VH-IVUS for use in the in vivo identification of plaque type.

Materials and methods

Animals

Sixteen New Zealand white male rabbits (2.0–2.5 kg, 4 months old), provided by the Experimental Animal Center of Fujian Medical University, were used in this study. Rabbits were individually housed in metal cages in a room maintained under controlled conditions with free access to water. Two rabbits in the experimental group died due to unrelated causes at six weeks after starting the high-fat diet. All experiments were approved by the ethics committee of Fujian Medical University in China. Experimental protocols conformed to the Guide for the Care and Use of Laboratory Animals published by the US National Institutes of Health (NIH Publication No. 85-23, revised 1996).

Experimental groups

After one week of adaptation to normal diet, the 16 rabbits were randomly divided into two groups: the control group ($n = 6$) was fed a 1% (high) fat diet and the experimental group ($n = 10$) was fed a high-fat diet combined with balloon injury to the aortic endothelium (at 2 weeks after starting the high-fat diet). The observation period was 12 weeks, after which VH-IVUS was performed on animals in the experimental group.

Balloon catheter injury

All rabbits in both groups were anaesthetized by intramuscular injection of ketamine (100 mg) and chlorpromazine (50 mg). After anaesthesia, the rabbits were fixed on the operating table. A longitudinal, 5-cm skin incision was made at the femoral region under local anaesthesia induced by 1% lidocaine hydrochloride. After incision, rabbits in the control group were sutured and returned to their cages.

In the experimental group, the right femoral artery was exposed. Under direct vision, rabbits underwent femoral artery puncture with a 24 G needle (paediatric anaesthesia). After successful puncture, a percutaneous transluminal coronary angioplasty guide wire was directly inserted. Under fluoroscopic guidance, a balloon catheter with a diameter of 3.0 mm was advanced to the upper abdominal aorta proximal to the left renal artery ostium. The balloon was inflated to maintain pressure at 0.606–1.01 MPa, and then slowly pulled back to the iliac arterial bifurcation. If the balloon was too small, then it was exchanged for a larger 0.5-mm balloon. The balloon was slowly pulled back to near the iliac artery (total length of about 8–10 cm) and deflated. The procedure was repeated three times without adverse event, and the surgical wounds were sutured.

VH-IVUS

Experimental group rabbits were anaesthetized by intramuscular injection of ketamine (100 mg) and chlorpromazine (50 mg). The right femoral artery was dissected under sterile conditions and under fluoroscopy. A 0.014-in angioplasty guidewire was advanced into the aorta. A phased-array IVUS catheter (20 MHz; Eagle Eye, Volcano Therapeutics Inc, Rancho Cordova, CA, USA) was positioned at the level of the left renal artery ostium of the abdominal aorta. Under continuous electrocardiogram monitoring, the IVUS catheter was pulled back at a continuous speed of 1 mm/s from the level of the renal artery of the abdominal aorta to the bifurcation of the aorta, and into the iliac arteries.

All IVUS images were digitized and stored on the hard disk of the IVUS console (Volcano Therapeutics Inc, Rancho Cordova, CA, USA) for spectral analysis of the backscattered radiofrequency signals. The VH-IVUS analysis gives a different colour code to fibrous (green), fibro-fatty (yellow-green), necrotic (red), and calcified (white) tissue. The predicted plaque composition is presented as a colour-coded tissue map. The different tissue components were expressed as the percentage of total plaque area ($=$ intimal $+$ medial area).

Lipid profile

Blood was drawn from overnight-fasted rabbits to measure the lipid profile at baseline (beginning of the study), after week 2 and after week 12 (termination of the experiment). Enzyme-linked immunosorbent assay was used to quantify the amount of different inflammation mediators, such as high sensitivity C-reactive protein (hs-CRP), matrix metalloproteinase-3 (MMP-3), interleukin (IL)-1, IL-10, tumour necrosis factor-α (TNF-α), and oxidized- low-density lipid (ox-LDL).

Histological examination

At the end of the experiment, the animals were euthanized by an overdose of pentobarbital. The left renal artery side branches of the abdominal aorta were marked with indelible ink (Bradley Products Inc, Bloomington, MN, USA). After the aorta was fixed in 4% formaldehyde (pH 7.4), a 5-cm length of the abdominal aorta was cut from the beginning of the left renal artery. The aorta was further sectioned into 3-mm rings. The tissue was dehydrated overnight and embedded in paraffin. Serial 5-μm cross-sections were stained with haematoxylin–eosin (H&E), Masson trichrome, von Kossa (which stains calcium salts), and Sirius red (which stains collagen fibre).

To identify the various tissue components, all images were analysed with a colour image analysis system (Image Pro Plus 6.0, Media Cybernetics Inc, Bethesda, MD, USA). The different tissue components were expressed as percentage of total plaque area. The following definitions for the different tissue components were used. Fibrous tissue was characterized by

bundles of collagen fibres with little or no lipid accumulation. Areas of loosely packed collagen bundles with interspersed extracellular lipid were labelled as fibro-fatty tissue. Necrotic core was defined as a hypocellular plaque cavity devoid of collagen and containing necrotic debris and cholesterol clefts. Calcified tissue was defined as compact calcium crystals, characterized by intense staining by H&E.

Accuracy of plaque-type identification by VH-IVUS

The histological staining results for the experimental group animals (133 tissue sections) were compared with 133 corresponding VH-IVUS images. To determine the accuracy of VH-IVUS for identification of the plaque type, every tissue section was compared to three consecutive frames of VH-IVUS. The following definitions for classification of atherosclerotic plaques by histology and VH-IVUS were used.[7,8] Pathological intimal thickening (PIT) was defined by histology and VH-IVUS as a mixture of mainly fibrous and fibro-fatty tissue, with limited amounts of microcalcification (<10% of plaque volume) and necrotic core (<10% of plaque volume). Fibroatheroma (FA) was defined by histology as a confluent necrotic core (>10% of plaque volume) covered by a thick (>150 μm) fibrous cap, and by VH-IVUS as a confluent necrotic core (>10% of plaque volume) with an overlying fibrous cap on three consecutive frames. Thin-cap FA (TCFA) was defined by histology as a confluent necrotic core (>10% of plaque volume) covered by a thin (<150 μm) fibrous cap, and by VH-IVUS as a confluent necrotic core (>10% of plaque volume) without an overlying fibrous cap (in direct contact with the lumen) on three consecutive frames.

If an FA or TCFA contained >10% dense calcium, then it was defined as calcified FA (FA-C) or calcified TCFA (TCFA-C), respectively. If an FA or TCFA did not contain >10% dense calcium, then it was defined as noncalcified FA (FA-NC) or noncalcified TCFA (TCFA-NC), respectively.

Table 1 Comparison of serum lipids levels between groups

		Control ($n=6$)	Experimental ($n=8$)	*P*
TC	Baseline	1.88 ± 0.06	1.85 ± 0.06	0.41
	Week 2	29.57 ± 0.54**	30.1 ± 1.63**	0.47
	Week 12	29.54 ± 0.64**	30.15 ± 1.59**	0.35
TG	Baseline	0.76 ± 0.05	0.78 ± 0.03	0.32
	Week 2	5.01 ± 0.17**	5.05 ± 0.34**	0.81
	Week 12	4.99 ± 0.14**	5.05 ± 0.37**	0.71
LDL-c	Baseline	0.73 ± 0.07	0.70 ± 0.08	0.49
	Week 2	24.63 ± 1.40**	25.35 ± 1.28**	0.34
	Week 12	27.9 ± 2.89#	29.13 ± 2.72##	0.43
HDL-C	Baseline	0.86 ± 0.05	0.88 ± 0.03	0.35
	Week 2	1.01 ± 0.07**	1.01 ± 0.07**	0.96
	Week 12	1.03 ± 0.04**	1.03 ± 0.05**	0.99

Experimental group was treated with high-fat diet + balloon injury; Control group was treated with high-fat diet alone. **$P < 0.01$ *vs*. baseline; #$P < 0.05$ *vs*. week 2; ##$P < 0.01$ *vs*. week 2.

Statistical analysis

Manual contour detection of the intimal and medial-adventitial boundaries was performed by two independent observers and the inter- and intra-observer variabilities were determined. Interobserver variability was measured by linear regression analysis.

All reported numeric data are expressed as means ± SD. Data were shown by 1-sample Kolmogorov-Smirnov test to

Table 2 Comparison of inflammatory cytokines between groups

		Control ($n=6$)	Experimental ($n=8$)	*P*
hs-CRP (μg/L)	Baseline	5.90 ± 0.52	6.14 ± 0.65	0.46
	Week 2	7.06 ± 0.26**	7.17 ± 0.62**	0.68
	Week 12	7.09 ± 0.38**	13.89 ± 4.01##	0.00
MMP-3 (μg/L)	Baseline	40.83 ± 11.24	46.19 ± 12.42	0.42
	Week 2	53.16 ± 4.79	53.52 ± 5.66	0.90
	Week 12	52.20 ± 5.00	67.56 ± 8.34##	0.00
IL-I (pg/mL)	Baseline	3339.45 ± 164.21	3290.88 ± 63.33	0.52
	Week 2	12,717.13 ± 579.52**	12,472.68 ± 253.54**	0.30
	Week 12	12,251.56 ± 468.48**	13,478.12 ± 864.28#	0.00
IL-10 (pg/mL)	Baseline	2664.49 ± 129.22	2709.83 ± 145.06	0.56
	Week 2	5877.90 ± 396.04**	5937.00 ± 293.07**	0.75
	Week 12	6284.59 ± 579.88**	12,966.29 ± 1281.42##	0.00
TNF-α (pg/mL)	Baseline	3351.51 ± 530.72	3488.99 ± 319.49	0.59
	Week 2	9083.95 ± 371.46**	8942.60 ± 351.82**	0.48
	Week 12	9527.63 ± 764.94**	11,338.53 ± 447.45##	0.00
ox-LDL(μg/L)	Baseline	71.38 ± 10.47	71.98 ± 3.53	0.88
	Week 2	320.74 ± 4.81**	319.88 ± 11.41**	0.85
	Week 12	314.79 ± 30.10**	429.79 ± 43.22##	0.00

Experimental group was treated with high-fat diet + balloon injury; Control group was treated with high-fat diet alone. **$P < 0.01$ *vs*. baseline; #$P < 0.05$ *vs*. week 2; ##$P < 0.01$ *vs*. week 2.

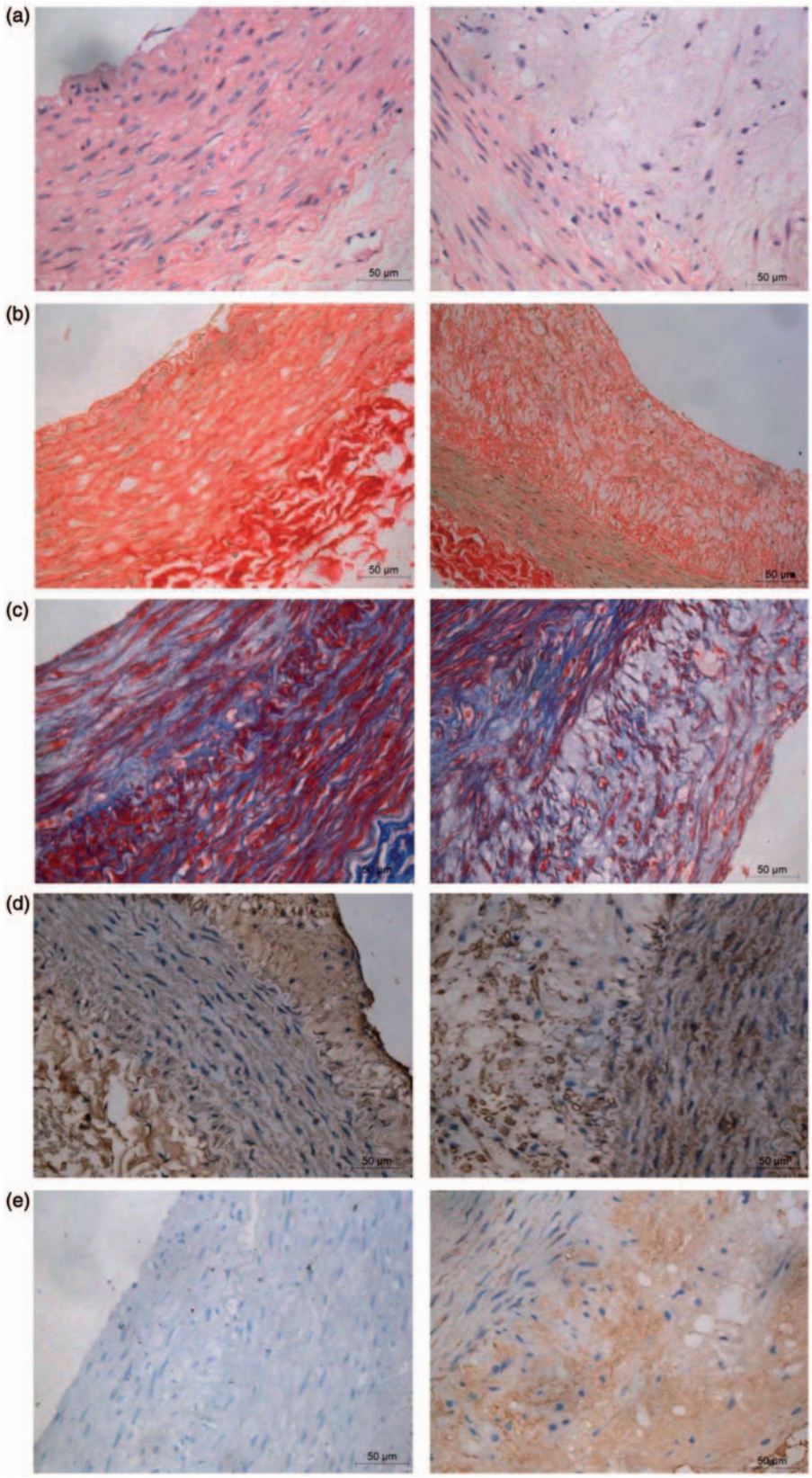

Figure 1 Staining with H&E (a), Sirius red (b), Masson trichrome (c), α-actin (d), and CD68 (e). All images are 10 × 40. Control (left) and experimental groups (right) are shown. Photomicrographs of aortic atherosclerotic plaque in experimental group showed extracellular lipids deposits, copious CD68-positive macrophages, and a thin fibrous cap. (A color version of this figure is available in the online journal)

Table 3 Comparison of histological results between groups

	Control ($n=6$)	Experimental ($n=8$)	*P*
Intramedia thickness (μm)	492.96 ± 45.21	487.98 ± 53.59	0.30
Plaque thickness (μm)	297.24 ± 24.20	552.60 ± 76.18	0.00
Fibrous cap thickness (μm)	168.79 ± 36.50	92.47 ± 16.70	0.00
Plaque thickness/ Intramedial thickness	60.67 ± 6.72	114.63 ± 20.42	0.00

Table 4 Comparison of immunohistochemical results between groups

	Control ($n=6$)	Experimental ($n=8$)	*P*
CD68	7.08 ± 1.91	19.03 ± 3.27	0.00
α-actin	10.91 ± 1.12	10.13 ± 0.9	<0.01

be normally distributed. Differences in continuous variables between two time periods were assessed by unpaired Student's t-test. For analysis of sensitivity, specificity, and positive predictive value (PPV), histology was used as the 'gold standard'.

Correlation between histology and VH-IVUS for the percent area of every tissue component (fibrous, fibro-fatty, necrotic calcified tissue, and confluent necrotic core) was

Table 6 Sensitivity, specificity, and positive predictive value (PPV) for identification of plaque type by VH-IVUS

Plaque type	Sensitivity (%)	Specificity (%)	PPV (%)
PIT, $n=63$	79.03	93.46	77.78
FA-NC, $n=93$	85.11	93.41	86.96
FA-C, $n=19$	89.47	97.67	73.91
TCFA-NC, $n=87$	87.36	97.35	93.83
TCFA-C, $n=14$	92.86	98.47	76.47

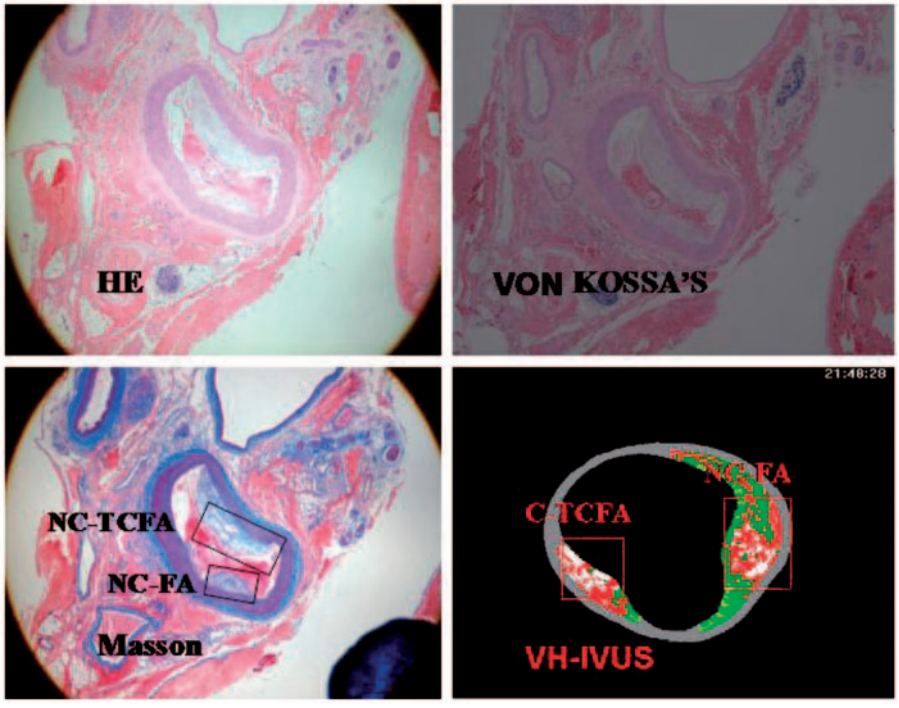

Figure 2 Correlation between histological and VH-IVUS data for areas represented by fibrous (a), fibro-fatty (b), necrotic calcified tissue (c), and confluent necrotic core (d). Left, linear regression shows a strong correlation between histology and VH-IVUS for different tissue components. Dashed lines represent 95% confidence limits. Right, the corresponding Bland-Altman plots are shown. The difference between histology and VH-IVUS did not vary in any systematic way over the range of measurements. The solid line denotes the mean difference, the dashed lines represent the 95% confidence limits. (A color version of this figure is available in the online journal)

Table 5 Comparison of plaque identification between histology and VH-IVUS

		VH-IVUS					
		PIT	FA-NC	FA-C	TCFA-NC	TCFA-C	Total
Histology	PIT	49	8	5	0	0	62
	FA-NC	8	80	0	5	1	94
	FA-C	1	0	17	0	1	19
	TCFA-NC	5	3	1	76	2	87
	TCFA-C	0	1	0	0	13	14

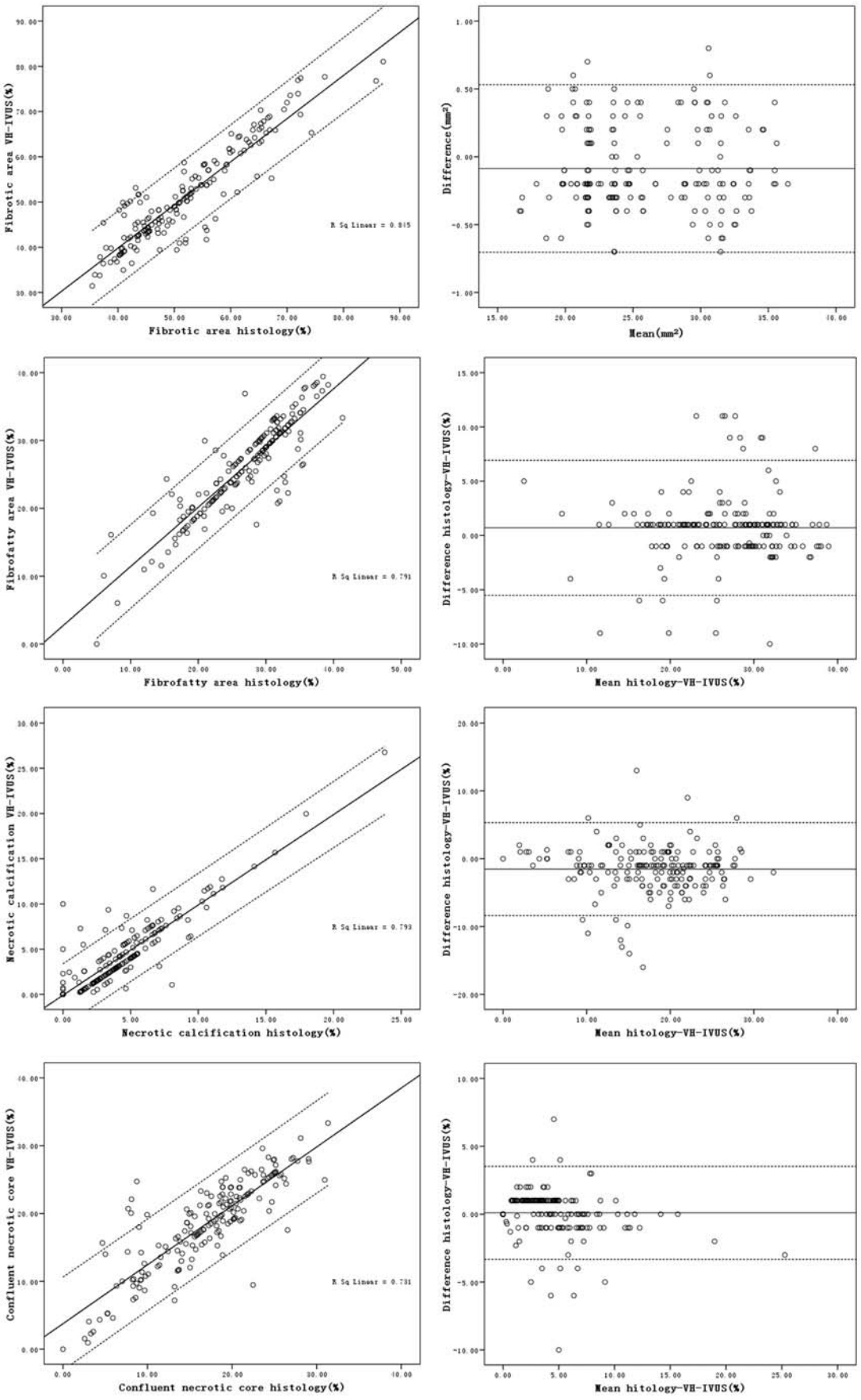

Figure 3 Staining of a plaque with H&E (a), von Kossa (b), and Masson trichrome (c) compared to results by VH-IVUS (d). Plaques were identified by histology as TCFA-NC and FA-NC, but were misdiagnosed by VH-IVUS as FA-NC and TCFA-C, respectively

evaluated by linear regression analysis and Bland-Altman plots, by plotting the difference in percent area of the different tissue components between histology and VH-IVUS versus the average percent area. Statistical analysis was performed with SPSS (v13.0, IBM, NY, USA). A P value of <0.05 was considered significant.

Results

Lipid profiles

Two rabbits in the experimental group died due to unrelated causes during the experiment. The serum lipid levels of all rabbits increased significantly after the high-fat diet, with further increase in LDL-C levels at week 12 as compared to week 2. These values did not significantly differ between the two groups (Table 1).

Inflammatory biomarkers

Levels of five inflammatory biomarkers (hs-CRP, IL-1, IL-10, TNF-α, and ox-LDL) of all rabbits were higher at week 2 than at baseline. The levels of hs-CRP, IL-1, IL-10, TNF-α, MMP-3, and ox-LDL of the experimental group were further increased at week 12 compared to values at week 2. Significant differences in the six biomarkers between the two groups were not found at baseline or week 2, but all six biomarkers were higher in the experimental group at week 12 (Table 2). This finding indicates that the inflammatory response after balloon injury involves vulnerable plaque formation.

Histological findings

Histological examination of the abdominal artery in the experimental group revealed extracellular lipid deposits, copious CD68-positive macrophages, and a thin fibrous cap, thus satisfying the conditions for a vulnerable plaque. In the control group, the artery showed copious fibrous tissue, marked hyperplasia of smooth muscle cells, and few lipid deposits (Figure 1). Differences between the two groups were found for the intramedia, plaque, and fibrous cap thicknesses, plaque thickness/intramedial thickness ratio (Table 3), and

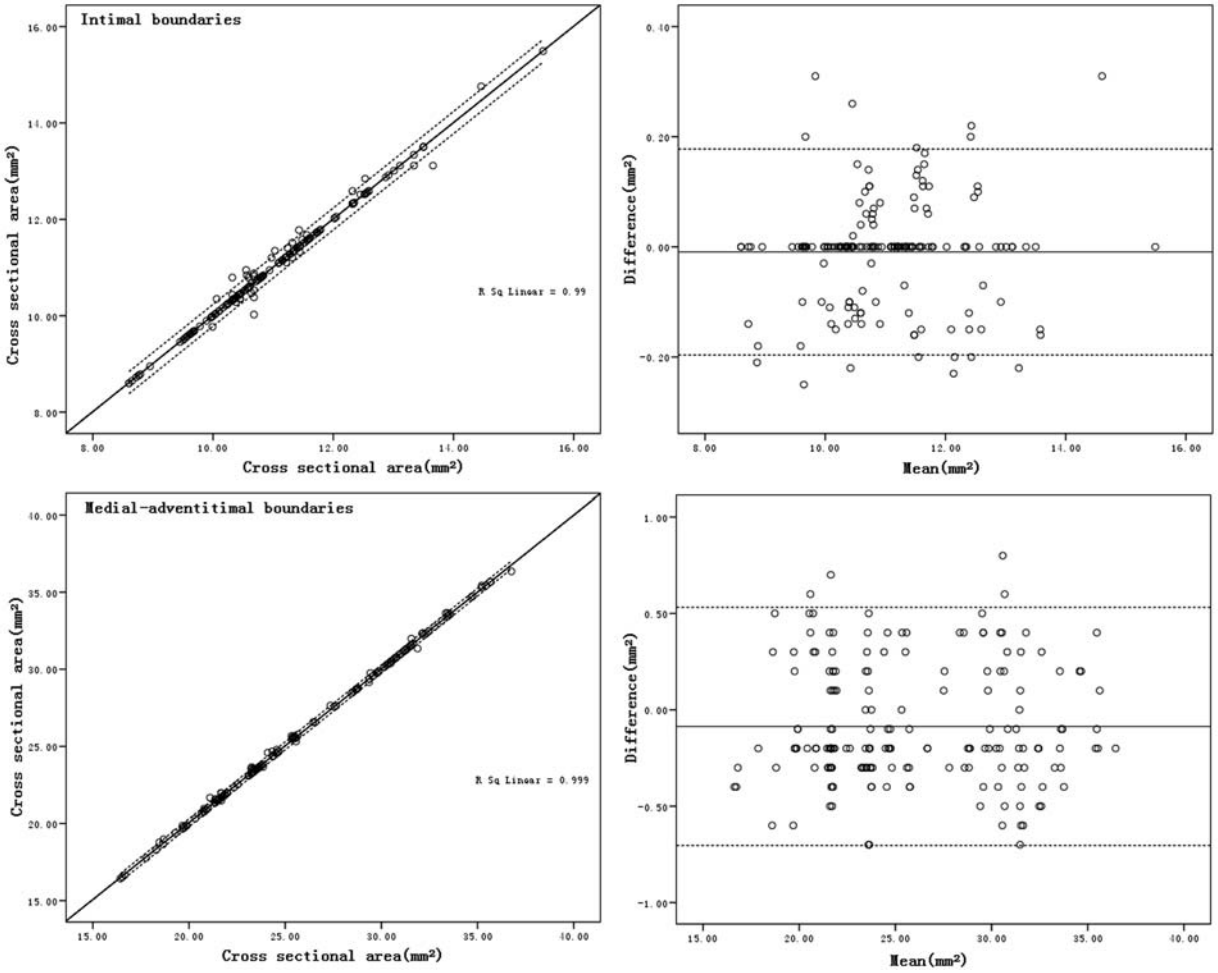

Figure 4 Intra-observer variability of intimal and medial-adventitial boundaries. Left, linear regression analysis shows a strong correlation between two measurements, which were performed by one observer with a four weeks interval. The dashed lines represent the 95% confidence limits. Right, the corresponding Bland-Altman plots are shown, which were constructed by plotting the difference between the two measurements versus the mean of both measurements. The solid line denotes the mean difference, the dashed lines represent the 95% confidence limits

positive staining for CD68 and α-actin (Table 4). Together, these results indicate that the vulnerable plaque animal model was successfully established and that balloon injury played an important role.

Comparison of histology with VH-IVUS

The findings of histology and VH-IVUS strongly correlated for the different tissue components. Linear regression analysis showed a strong correlation between histology and VH-IVUS for the percent area of fibrous tissue ($R = 0.845$, $P < 0.001$), fibro-fatty tissue ($R = 0.791$, $P < 0.001$), necrotic calcified tissue ($R = 0.793$, $P < 0.001$), and confluent necrotic core ($R = 0.731$, $P < 0.001$; Figure 2).

A total of 276 atherosclerotic plaques were analysed. The sensitivity, specificity, and PPV for the different plaque types are summarized in Tables 5 and 6. VH-IVUS performed best in the identification of TCFA-NC and TCFA-C, with high sensitivity (87.36% and 92.86%, respectively) and specificity (97.35% and 98.47%, respectively). The PPV was high for TCFA-C (93.83%) but low for TCFA-NC (76.47%). VH-IVUS misdiagnosed 5.88% of FA-NC, 5.88% of FA-C, and 11.76% of TCFA-NC lesions as TCFA-C (Figure 3). VH-IVUS correctly identified 85.11% and 89.47% of FA-NC and FA-C, respectively, but misdiagnosed 5.32% of FA-NC as TCFA-NC, which indicates that VH-IVUS underestimated the fibrous cap thickness. Furthermore, 12.9% and 8.06% of PIT were misdiagnosed as FA-NC and FA-C, respectively, which suggests that the PIT foam cells were misclassified as necrotic or calcified tissue. VH-IVUS showed a sensitivity of 79.03% and PPV of 77.78% for PIT detection.

Interobserver variability

The intra-observer and inter-observer variabilities of the intimal and medial-adventitial boundaries were low (Figures 4 and 5). For intra-observer variability, coefficient of variance (CV) analysis showed (0.103, 0.102) for the luminal area and (0.191, 0.191) for the vessel area. For inter-observer variability, CV analysis showed (0.102, 0.101) for the luminal area and (0.190, 0.190) for the vessel area.

Discussion

According to the histological results of the present study, the abdominal artery plaque induced by high-fat diet + balloon injury in rabbits satisfied the three features of a 'vulnerable plaque': it had a lipid rich core, accumulation of macrophages,

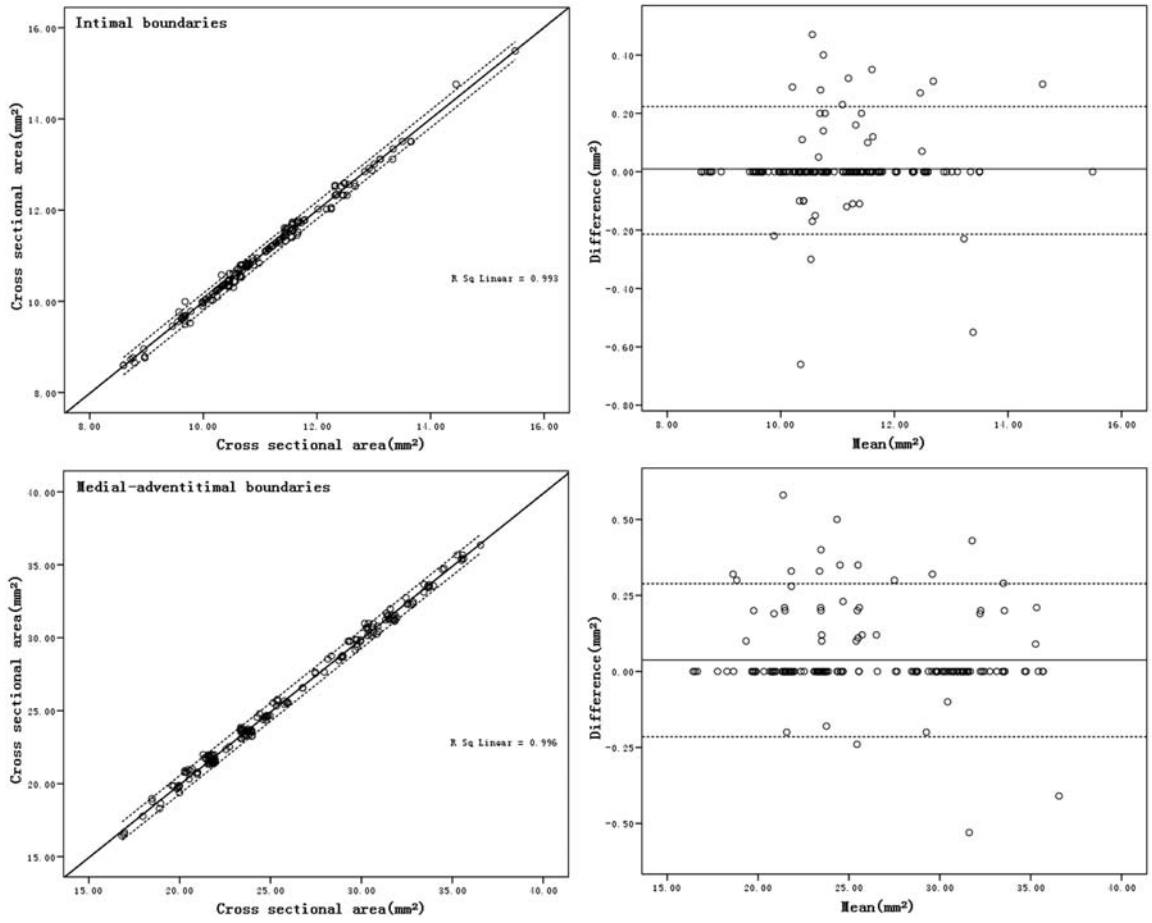

Figure 5 Inter-observer variability of intimal (a) and medial-adventitial (b**B**) boundaries. Left, the linear regression analysis shows strong correlation between two measurements, which were performed by two observers. Dashed lines represent 95% confidence limits. Right, the corresponding Bland-Altman plots are shown, which were constructed by plotting the difference between the two measurements versus the mean of both measurements. The solid line denotes the mean difference, the dashed lines represent the 95% confidence limits

and a thin fibrous cap. This finding indicates that we have successfully established a vulnerable plaque animal model in our experimental group. Presence of the endothelial balloon injury affected the histological characteristics of the formed plaque. This finding is distinct from those of Shimizu et al., who found that cholesterol content and presence of endothelial injury have no effect on the histological characteristics of the formed plaque.[9]

We observed a high accuracy of VH-IVUS for the in vivo identification of plaque type in a rabbit model of AS. VH-IVUS not only provided high sensitivity, specificity, and PPV for the detection of TCFA-NC, but also had good sensitivity and specificity for the detection of PIT, TCFA-C, FA-NC, and FA-C, consistent with the findings of Van Herck et al.[10] In contrast, compared to Van Herck et al., we observed fewer FA-C and TCFA-C lesions and obtained poorer PPV results for those lesions (73.91% and 76.47%, respectively). Use of the shorter time in our study (12 weeks vs. 12–18 months in Ref. 10) to establish animal models resulted in the large accumulation of foam cells and little calcified component in the atherosclerotic plaques. Foam cells, which are found in atherosclerotic plaques of animal models[11,12] and in humans,[13] were misclassified by VH-IVUS as necrotic or calcified tissue, leading to incorrect determination of plaque type.

Linear regression analysis showed a good correlation between histology and VH-IVUS for fibrotic, fibro-fatty and necrotic calcified tissue, consistent with previous studies.[14,15] In addition, there was a strong correlation between histology and VH-IVUS for the percent area of the confluent necrotic core, indicating that VH-IVUS measurements of the plaque composition are reproducible.

VH-IVUS has several limitations, including a limited axial resolution. Our definition of VH-IVUS-derived TCFA differed from that of histologically defined TCFA, the latter of which involved a critical fibrous cap thickness of 65 μm. Thus, 'absence' of a fibrous cap implies that the fibrous cap is <150-μm thick; it may not be truly 'pathologically thin'. At present, the exact value of VH-IVUS-derived TCFA for predicting future cardiovascular events is unknown. Our model does not include diverging vessels such as the carotid and coronary arteries, and it could not determine whether the plaque had characteristics of histological vulnerability to rupture. Finally, to save expense, we only evaluated the value of VH-IVUS in the experimental group.

Despite these limitations, our results show that the model of vulnerable plaque in New Zealand white rabbit abdominal aorta established by high-fat diet + balloon injury is portable and useful. Longitudinal studies examining the effect of interventions on the vulnerable plaque model through VH-IVUS are possible.

Author contributions: All authors participated in the design of the studies, analysis of the data and review of the manuscript.

ACKNOWLEDGEMENTS

The authors thank the catheterization laboratory staff for their enthusiasm in supporting the study. This study was supported by the Natural Science Foundation of China (No. 81070165) and the Natural Science Foundation of Fujian Province of China (No. 2010J05064).

REFERENCES

1. Cullen P, Baetta R, Bellosta S, Bernini F, Chinetti G, Cignarella A, von Eckardstein A, Exley A, Goddard M, Hofker M, Hurt-Camejo E, Kanters E, Kovanen P, Lorkowski S, McPheat W, Pentikäinen M, Rauterberg J, Ritchie A, Staels B, Weitkamp B, de Winther M. MAFAPS Consortium Rupture of the atherosclerotic plaque: does a good animal model exist? Arterioscler Thromb Vasc Biol 2003;23:535–42
2. Abela GS, Picon PD, Friedl SE, Gebara OC, Miyamoto A, Federman M, Tofler GH, Muller JE. Triggering of plaque disruption and arterial thrombosis in an atherosclerotic rabbit model. Circulation 1995;91:776–84
3. Gertz SD, Fallon JT, Gallo R, Taubman MB, Banai S, Barry WL, Gimple LW, Nemerson Y, Thiruvikraman S, Naidu SS, Chesebro JH, Fuster V, Sarembock IJ, Badimon JJ. Hirudin reduces tissue factor expression in neointima after balloon injury in rabbit femoral and porcine coronary arteries. Circulation 1998;98:580–7
4. Rekhter MD, Hicks GW, Brammer DW, Work CW, Kim JS, Gordon D, Keiser JA, Ryan MJ. Animal model that mimics atherosclerotic plaque rupture. Circ Res 1998;83:705–13
5. Rekhter MD. How to evaluate plaque vulnerability in animal models of atherosclerosis? Cardiovasc Res 2002;54:36–41
6. Rodriguez-Granillo GA, Vaina S, Garcia-Garcia HM, Valgimigli M, Duckers E, van Geuns RJ, Regar E, van der Giessen WJ, Bressers M, Goedhart D, Morel MA, de Feyter PJ, Serruys PW. Reproducibility of intravascular ultrasound radiofrequency data analysis: implications for the design of longitudinal studies. Int J Cardiovasc Imaging 2006;22:621–31
7. García-García H, Goedhart D, Schuurbiers JC, Kukreja N, Tanimoto S, Daemen J, Morel MA, Bressers M, van Es GA, Wentzel JJ, Gijsen F, van der Steen AF, Serruys PW. Virtual histology and remodelling index allow in vivo identification of allegedly high-risk coronary plaques in patients with acute coronary syndromes: a three vessel intravascular ultra-sound radiofrequency data analysis. EuroIntervention 2006;2:338–44
8. Konig A, Margolis MP, Virmani R, Holmes D, Klauss V. Technology Insight: in vivo coronary plaque classification by intravascular ultrasonography radiofrequency analysis. Nat Clin Pract Cardiovasc Med 2008;5:219–29
9. Shimizu T, Nakai K, Morimoto Y, Ishihara M, Oishi H, Kikuchi M, Arai H. Simple rabbit model of vulnerable atherosclerotic plaque. Neurol Med Chir (Tokyo) 2009;49:327–32
10. Van Herck J, De Meyer G, Ennekens G, Van Herck P, Herman A, Vrints C. Validation of in vivo plaque characterisation by virtual histology in a rabbit model of atherosclerosis. EuroIntervention 2009;5:149–56
11. Barbolini G, Scilabra GA, Botticelli A, Botticelli S. On the origin of foam cells in cholesterol-induced atherosclerosis of the rabbit. Virchows Arch B Cell Pathol 1969;3:24–32
12. Coleman R, Hayek T, Keidar S, Aviram M. A mouse model for human atherosclerosis: long-term histopathological study of lesion development in the aortic arch of apolipoprotein E-deficient (E0) mice. Acta Histochem 2006;108:415–24
13. Kockx MM, De Meyer GR, Bortier H, de Meyere N, Muhring J, Bakker A, Jacob W, Van Vaeck L, Herman A. Luminal foam cell accumuation is associated with smooth muscle cell death in the intimal thickening of human saphenous vein grafts. Circulation 1996;94:1255–62
14. Nair A, Margolis M, Kuban B, Vince DG. Automated coronary plaque characterisation with intravascular ultrasound backscatter: ex vivo validation. EuroIntervention 2007;3:113–20
15. Nasu K, Tsuchikane E, Katoh O, Vince DG, Virmani R, Surmely JF, Murata A, Takeda Y, Ito T, Ehara M, Matsubara T, Terashima M, Suzuki T. Accuracy of in vivo coronary plaque morphology assessment: a validation study of in vivo virtual histology compared with in vitro histopathology. J Am Coll Cardiol 2006;47:2405–12

(Received February 15, 2012, Accepted February 19, 2013)